Non-genetic adaptation by collective migration

Lam Vo[1,2,*], Fotios Avgidis[3,*], Henry H. Mattingly[4,*], Ravi Balasubramanian[1], Thomas S. Shimizu[3], Barbara I. Kazmierczak[5], Thierry Emonet[1,2,6,#]

Author affiliations: [1] Department of Molecular, Cellular, and Developmental Biology, Yale University, New Haven, CT; [2] Quantitative Biology Institute, Yale University, New Haven, CT; [3] AMOLF Institute, Amsterdam, The Netherlands; [4] Center for Computational Biology, Flatiron Institute, New York, NY; [5] Department of Medicine & Microbial Pathogenesis, Yale University, New Haven, CT; [6] Department of Physics, Yale University, New Haven, CT

* These authors contributed equally to this work

[#] To whom correspondence may be addressed

Email: thierry.emonet@yale.edu

Abstract

Collective behaviors require coordination of individuals. Thus, a population must adjust its phenotypic distribution to adapt to changing environments. How can a population regulate its phenotypic distribution? One strategy is to utilize specialized networks for gene regulation and maintaining distinct phenotypic subsets. Another involves genetic mutations, which can be augmented by stress-response pathways. Here, we studied how a migrating bacterial population regulates its phenotypic distribution to traverse across diverse environments. We generated isogenic *Escherichia coli* populations with varying distributions of swimming behaviors and observed their phenotype distributions during migration in liquid and porous environments. Surprisingly, we found that during collective migration, the distributions of swimming phenotypes adapt to the environment without mutations or gene regulation. Instead, adaptation is caused by the dynamic and reversible enrichment of high-performing swimming phenotypes within each environment. This adaptation mechanism is supported by a recent theoretical study, which proposed that the phenotypic composition of a migrating population results from a balance between cell growth generating diversity and collective migration eliminating the phenotypes that are unable to keep up with the migrating group. Furthermore, by examining chemoreceptor abundance distributions during migration towards different attractants, we found that this mechanism acts on multiple chemotaxis-related traits simultaneously. Our findings reveal that collective migration itself can enable cell populations with continuous, multi-dimensional phenotypes to flexibly and rapidly adapt their phenotypic composition to diverse environmental conditions.

Significance statement

Conventional cell adaptation mechanisms, like gene regulation and random phenotypic switching, act swiftly but are limited to a few traits, while mutation-driven adaptations unfold slowly. By quantifying phenotypic diversity during bacterial collective migration, we discovered an adaptation mechanism that rapidly and reversibly adjusts multiple traits simultaneously. By dynamically

balancing the elimination of phenotypes unable to keep pace with generation of diversity through growth, this process enables populations to tune their phenotypic composition based on the environment, without the need for gene regulation or mutations. Given the prevalence of collective migration in microbes, cancers, and embryonic development, non-genetic adaptation through collective migration may be a universal mechanism for populations to navigate diverse environments, offering insights into broader applications across various fields.

Introduction

Collective behaviors require that a population coordinates individuals with different phenotypes[1-3]. On top of this, they often must perform the collective behavior in different contexts[4], where different phenotypes might be advantageous. Both challenges can be addressed if the population regulates its phenotypic composition.

One strategy for adapting a population's phenotypic distribution involves controlling gene expression or maintaining distinct phenotypic states[5,6]. A classic example is persister formation, where bacteria[7-9] or cancer cells[10] randomly transition into antibiotic-resistant or chemotherapy-tolerant states. However, these rely on specialized regulatory networks and can only switch a few phenotypes among discrete states[11,12]. Alternatively, another strategy involves acquiring mutations, such as in bacterial efflux pumps[13,14] or the binding sites of EGFR[15] in cancer cells, to evade stressors. Nevertheless, this adaptation mode is slow, typically occurring at the timescale of tens of generations[16-18].

Here, we examined whether and how a migrating bacterial population regulates Its phenotypic composition according to environments it encounters. Groups of *Escherichia coli* cells can collectively migrate by consuming attractant cues in their environments and chasing the traveling gradient that they create[1]. Individual cells within the migrating group exhibit varying tumble biases, or TBs (**Fig. 1a**), and chemoreceptor abundances (**Fig. 1b**), leading to differences in the speeds at which they climb the attractant gradients[3]. These cells can travel together by spatially organizing within the migrating group such that their gradient-climbing abilities match the local steepness of the attractant gradient[1] (**Fig. 1c**). However, this spatial sorting mechanism is imperfect: cells at the back, or the low performers, slowly fall behind the migrating population because the attractant concentration falls below the detection limit of their receptors[1]. To maintain migration, the lost cells must be replaced through cell divisions[4].

Can a migrating bacterial population adapt its phenotypic composition without relying on gene regulation or mutations? A recent theoretical model[4] proposed that the dynamic balance between the loss of low-performing phenotypes and growth could be sufficient to adapt the population's composition to new environments. The elimination of weak phenotypes by collective migration[1] and production of new phenotypes by growth[19] would balance out such that the traveling population becomes enriched with "fitter" phenotypes—those with higher chemotactic performance—increasing its expansion speed[4]. Since the demands of migration are different in different environments, which phenotypes are enriched depends on the environment the population traverses[4] (**Fig. 1d**). However, this model has never been experimentally tested.

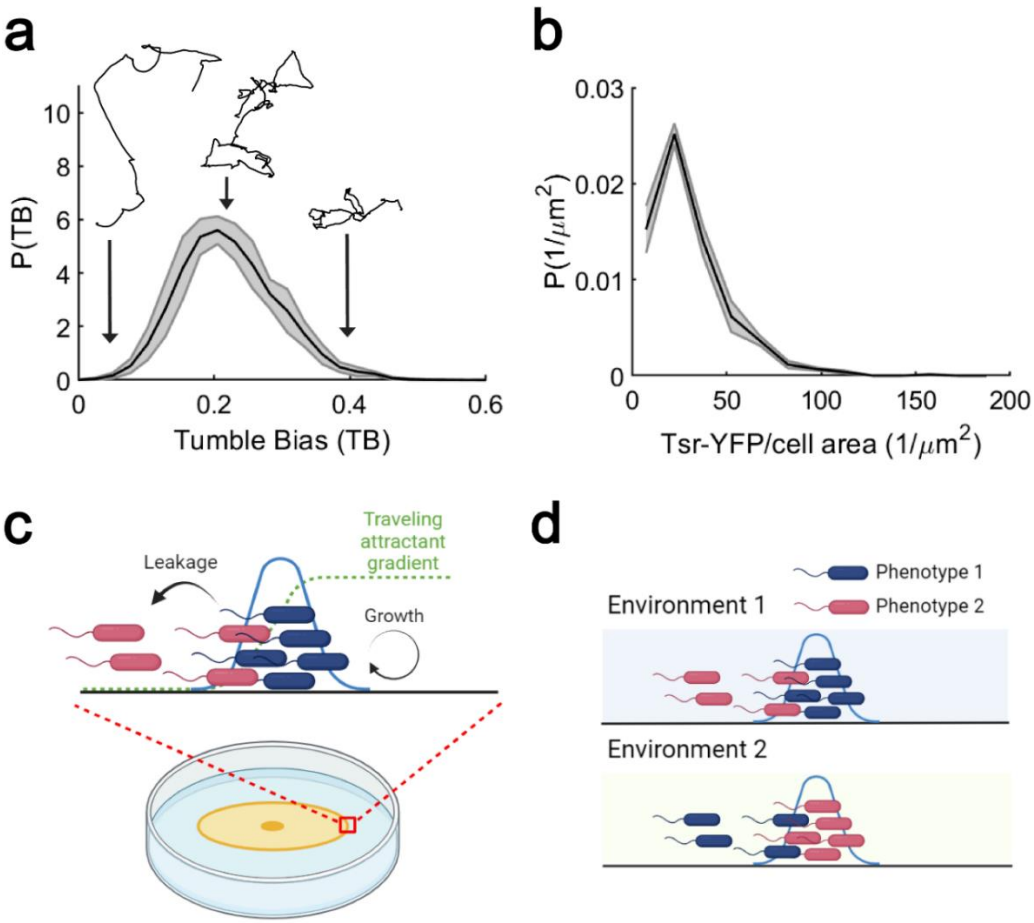

Figure 1: Isogenic populations of bacteria exhibit diversity in behavioral and sensory phenotypes while performing collective migration. (a) *In an isogenic population of E. coli**,** there is diversity in swimming behaviors, which can be quantified, for example, by measuring tumble bias in E. coli RP437 ($N_{rep} = 3$, N_{cells} = 9417).* ***(b)*** *There is also diversity in sensory ability, which correlates with variations in Tsr levels (as measured in E. coli MG1655, $N_{rep} = 3$, N_{cells} = 1695).* ***(c)*** *Under nutrient-replete conditions, cells consume attractants and collectively migrate using the resulting traveling attractant gradients[20]. During this process, cells spatially organize based on their ability to climb the traveling gradients[1]. Cells with higher chemotactic performances lead at the front, while cells with lower chemotactic performances travel at the back and eventually fall behind the migrating group. In such nutrient-replete conditions, cells continue to divide and generate diversity by replenishing phenotypes.* ***(d)*** *Theory predicts[4] that the balance between environment-dependent cell loss and growth enables the migrating isogenic population to dynamically tune its phenotypic composition to the environments it traverses.*

Here, we experimentally demonstrate this novel adaptation mechanism. By measuring the migrating population's distribution of swimming behaviors during migration in liquid and agarose, we observed that the migrating *E. coli* population tunes its own distribution of swimming behaviors, without relying on gene regulation or mutation. Instead, adaptation relies on differential loss of low-performing swimming phenotypes during migration in each environment. Furthermore, by examining the population's distributions of chemoreceptor abundances during migration

toward different attractants, we found that this mechanism acts on multiple chemotaxis-related traits simultaneously. More broadly, migration and other collective behaviors may generically provide rapid and flexible ways for diverse populations to adapt to changing conditions.

Results

Collective migration tunes the population's distribution of swimming phenotypes

First, we investigated whether the TB distribution of an *E. coli* population can be adapted during collective migration with growth. Given that some swimming phenotypes are better at navigating as a group than others[1], we expected that the TB distribution of a population, regardless of its starting point, to enrich for high-performing TBs and shift toward an "optimal" distribution during collective migration. To test this hypothesis, our approach was to propagate migrating waves using populations of cells with distinct initial TB distributions. Populations with different initial TB distributions were generated by controlling the expression levels of the phosphatase CheZ using an inducible promoter in cells lacking the endogenous *cheZ* gene, as done before[1,16,21] (**Methods**). Growing this strain with a high concentration (16 ng/mL) or low concentration (2 ng/mL) of the inducer, anhydrotetracycline (aTc), resulted in a population with low average TB or high average TB, respectively (**Fig. S1**). Wild type (WT) *E. coli* has a TB distribution that is between these two extremes (**Fig. 1a**).

To propagate migrating waves of growing bacteria, we utilized the classic swim plate assay[22], in which cells migrate through a fibrous mesh of 0.14% w/v semisolid agarose[22]. We inoculated *E. coli* populations with different initial TB distributions at the center of agarose swim plates, let them migrate for 15 hours, collected cells at the edge of the expanding colonies ("wave"), and measured their TB distributions by transferring the cells to a liquid environment and tracking single cells under a microscope. In parallel, we grew populations with the same inducer concentrations in shaking flasks ("batch") and measured their TB distributions (**Fig. 2a**). aTc degrades over time; therefore, we aged the aTc before adding it to the batch culture growth medium to mimic the conditions in the migrating wave (**Fig. S2; Methods**). The same experiments were performed with WT cells in the absence of aTc. By comparing the TB distributions of populations that migrated on the plates with those grown in batch culture, we quantified the effect of collective migration on the populations' TB distributions.

We found that the TB distribution of the high-TB population (initial mean TB = 0.32 ± 0.012, uncertainties throughout are the standard deviation of the mean across biological replicates) shifted toward lower TBs (final mean TB = 0.23 ± 0.026) during migration on plates (**Fig. 2e**). In this population, cells with lower TB were enriched, while cells with high TB were filtered out (**Fig. 2h**). Conversely, the TB distribution of the low-TB population (initial mean TB = 0.10 ± 0.011) shifted to higher TBs (final mean TB = 0.18 ± 0.0061) after migration on the plates (**Fig. 2c**). In this case, the enrichment was opposite: cells with low TB were filtered out, while cells with higher TB were enriched (**Fig. 2f**). In both cases, the populations became enriched for cells with intermediate TBs close to ~0.2, which happens to be the mean TB of wild-type populations grown in batch culture (mean TB = 0.22 ± 0.029) (**Fig. S3)**. Consistent with these observations, the TB distribution of the migrating WT population (final mean TB = 0.22 ± 0.012) was similar to its batch culture distribution (**Fig. 2d,g**). All changes in the mean TB during migration were statistically significant, as measured by two-sided T-test, except that of the WT population.

We measured the expansion speeds of the three populations on agarose swim plates to quantify how these shifts in phenotype composition affected migration speed (**Methods; Fig. 2b**). We found that the WT population (mean expansion speed 0.174 ± 0.007 mm/min) and the high-TB population (0.170 ± 0.02 mm/min) expanded the fastest (difference in speed was not statistically significant), whereas the low-TB population was slower (0.150 ± 0.02 mm/min; significant to $P < 0.005$). This suggests that the initial TB distribution of the WT population is positioned near the optimal phenotype for migrating through the semisolid agarose environment we used. The growth rates of WT, low-TB, and high-TB populations are similar (**Fig. S4**), therefore the differences in their expansion speeds are solely due to differences in chemotactic performance. Since the TB distributions of low-TB and high-TB populations shifted toward the TB distribution of the WT population (**Fig. S3)**, this suggests that collective migration enriches for high-performing phenotypes.

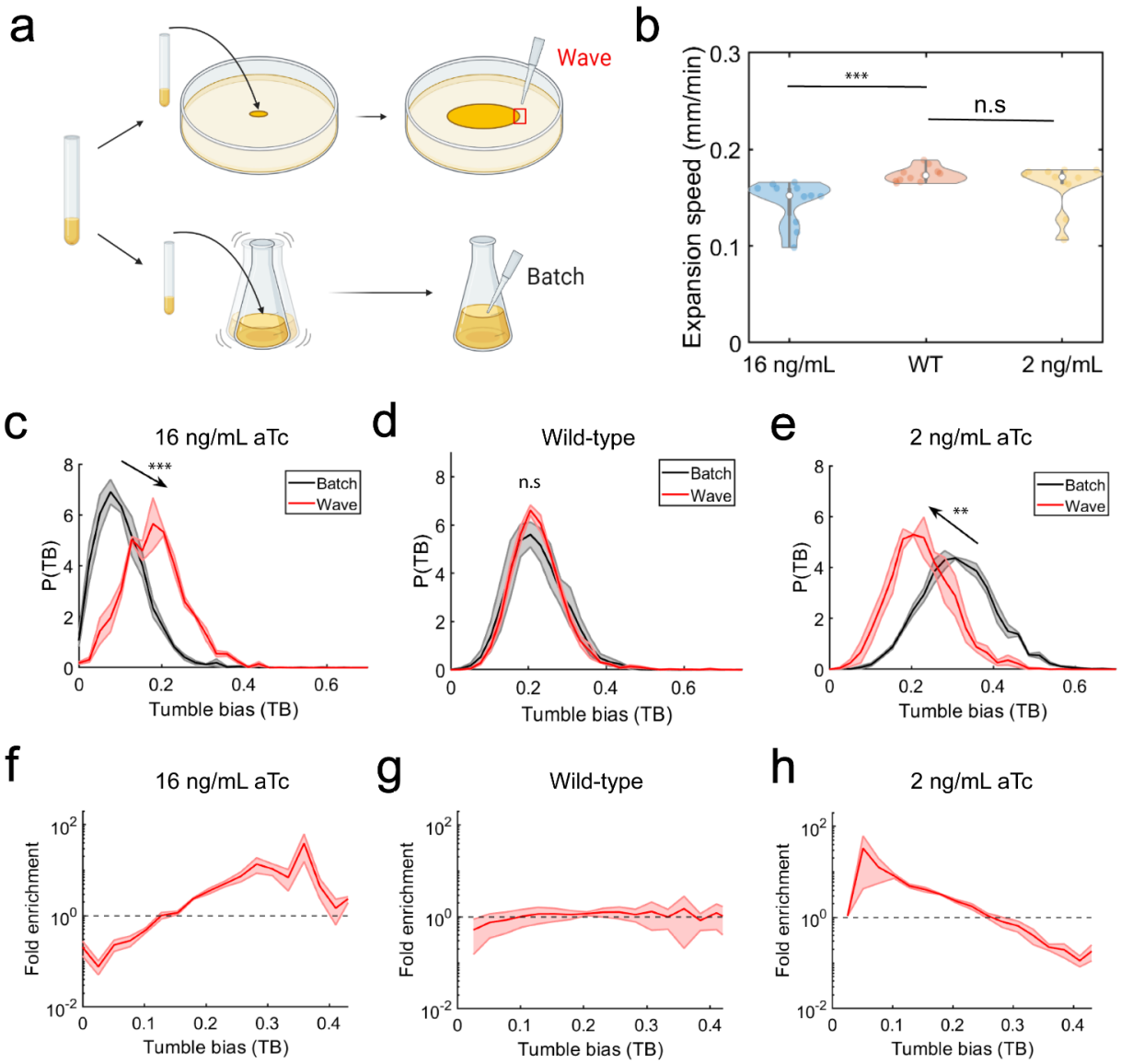

***Figure 2**. **Migration in agarose swim plate tunes TB distribution of the population: (a)** Experimental design: a swim plate and shaking flask containing the same amount of inducer are inoculated with the same initial population. TB distributions are measured and compared between batch and the migrating ring ("wave") after spending the same amount of time in either condition. **(b)** Expansion speeds of RP437 wild-type (mean expansion speed 0.174 ± 0.0077 mm/min; uncertainties throughout the paper are the standard deviation of the mean across replicates; here, $N_{rep} = 5$), ΔcheZ (pTet-CheZ) induced with 2 ng/mL aTc (mean 0.169 ± 0.02 mm/min; $N_{rep} = 5$), and 16 ng/mL (mean 0.145 ± 0.022 mm/min; $N_{rep} = 5$) populations on agarose swim plates (N=5). Two-sided T-tests were performed throughout to determine significance of the difference between pairs of means throughout (throughout, *** = P<0.0005, ** = P<0.005, * = P<0.05, and n.s. = not significant). **(c)** Populations with low initial mean TB (mean TB = 0.10 ± 0.01; $N_{rep} = 3$, $N_{cells} = 21{,}891$) shift toward a higher mean TB after migration on the plates (0.18 ± 0.01; $N_{rep} = 3, N_{cells} = 5{,}103$). Shaded area on the TB distribution is the standard error of the mean probability in each TB bin. Significance here refers to change in the mean of the distribution. **(d)** There was minimal or no shift in wild-type population's TB distribution during collective migration on the plates (0.22 ± 0.01; $N_{rep} = 4$, $N_{cells} = 15{,}774\ cells$) compared to batch culture (0.22 ± 0.03; $N_{rep} = 3$, $N_{cells} = 9{,}417$). **(e)** On the other hand, populations with high initial mean TB (0.31 ± 0.01; $N_{rep} = 3$, $N_{cells} = 26254$) shifted toward a lower mean TB after migration (0.23 ± 0.03; $N_{rep} = 3, N_{cells} = 6951$). **(f)** When low TB populations migrated on the plates**,** fold enrichment of cells with high TB is observed, while cells with low TB are filtered out ($N_{rep} = 3$). Shaded area on the fold-enrichment throughout is the standard errors of the mean enrichment values within each TB bin **(g)**. No enrichment and filtering of TB were observed in wild-type populations ($N_{rep} = 3$). **(f)** When high TB populations migrated on the plates**,** enrichment of cells with low TB is observed, while cells with high TB are filtered out ($N_{rep} = 3$).*

Tuning of swimming phenotype distributions is non-genetic and occurs without change in CheYZ expression

What is the mechanism that enables a migrating bacterial population to tune its TB distribution? Our recent theory predicts that the tuning of phenotypic distributions is a dynamic, non-genetic process mediated by the loss of low-performing chemotaxis phenotypes[1] and production of new phenotypes through growth[4,19]. However, during our swim plate assays, cells in the migrating populations could potentially acquire mutations that permanently alter their swimming behaviors[16-18]. If TB tuning is non-genetic, then we expect that the TB distributions of cells in the migrating waves would go back to their initial TB distributions when grown in batch culture.

To test this hypothesis, we isolated cells from the edge of the low- and high-TB migrating colonies on agarose swim plates, grew them in batch culture with aged aTc, and measured their TB distributions after growth (**Fig. 3a**). We found that the TB distributions of migrating bacterial populations went back to their initial TB distributions after re-growth in batch culture, suggesting that the cells in the migrating population did not acquire mutations that would have permanently altered their swimming behaviors (**Fig. 3b, c**).

Even without mutations, the shifts in TB distribution that we observed during migration could have been caused by changes in gene expression. Chemotaxis is regulated during *E. coli* growth, leading to changes in a population's TB distribution at different growth phases[23]. Manipulating the levels of response regulator CheY and its phosphatase CheZ is well-established to change TB[3], thus we assessed whether the shifts in TB distributions were due to changes in *cheY* and *cheZ* expressions. We measured the protein expression levels of CheY and CheZ by fusing them to fluorescent proteins (RFP and YFP, respectively) at their native chromosomal loci in a non-motile

strain. This non-motile strain acted as a biosensor for any change in the environment that would perturb CheYZ expression. We spread these cells uniformly on agarose swim plates, initiated migrating waves of motile, unlabeled WT cells at the center of the plates, and then picked cells from both the center and the edge of the migrating colonies (**Methods**). As the WT cells migrated, consuming the nutrients on the plate and forming spatial gradients of attractant, the non-motile biosensing cells experienced the same local environment as migrating cells. The distributions of CheY and CheZ protein expression levels in cells from the two locations, measured using fluorescent microscopy (**Methods**), showed no differences (**Fig. S5**). This indicated that *cheY* and *cheZ* expression levels did not change during collective migration.

Together, these observations indicate that the tuning of TB distributions is highly unlikely to be mediated by gene regulation or mutations.

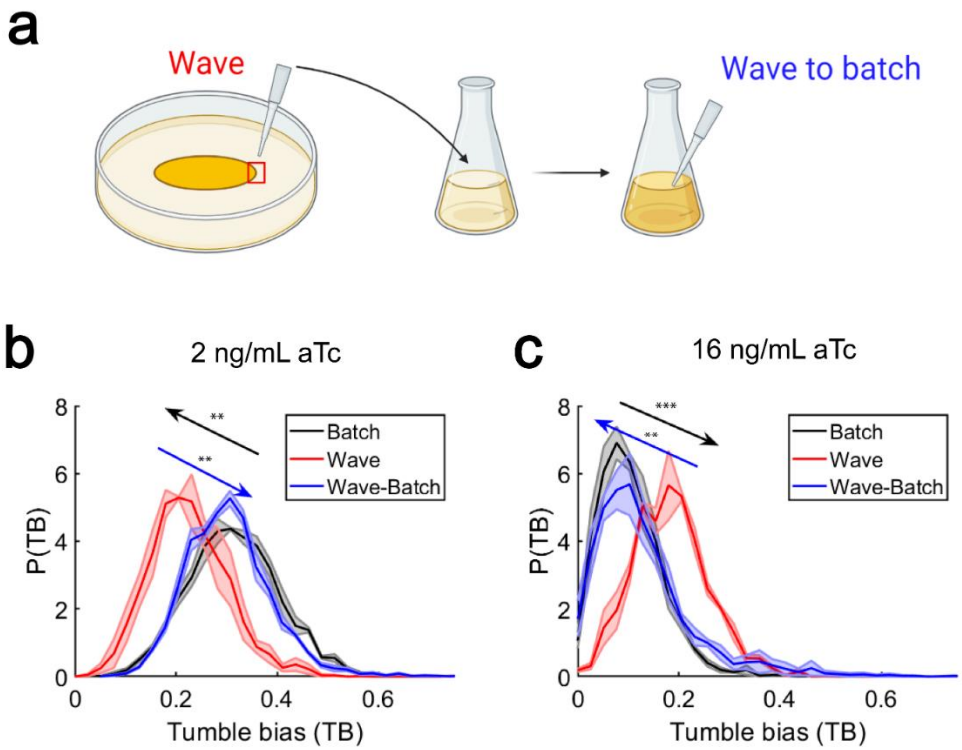

Figure 3: Tuning of TB by collective migration is reversible. (a) *To determine whether the tuning of TB becomes fixed or remains adaptable, we isolated cells from the edge of the migrating colonies ("wave"), grew the cells in liquid batch culture until exponential phase, and measured the TB distributions after growth ("wave-batch").* ***(b)*** *Black and red are the TB distributions of populations with high initial TB before and after migrating on agarose swim plates (same data as Fig. 2c). Blue: TB distribution of cells that migrated (red) after regrowth in batch culture (mean TB = 0.30 ± 0.01;* $N_{rep} = 3, N_{cells} = 15{,}774$*). The TB distributions of the populations that migrated on agarose swim plates, after growing in flasks, shifted back to the original batch culture's distributions.* ***(c)*** *Same as B, the TB distributions of populations with low initial TB, after growing in flask, (0.13 ± 0.021;* $N_{rep} = 3$, $N_{cells} = 20{,}403$*) shifted back to the TB distributions observed in batch culture (black and red are same as in Fig. 2c). The mean values of "batch" and "wave-batch" TB distributions in both cases are not significantly different.*

Tuning of swimming phenotype distributions adapts the population to the physical environment

So far, we have shown that migrating cell populations can non-genetically tune their own phenotypic compositions. Furthermore, we argue that this tuning enriches the population for high-performing chemotaxis phenotypes. If this is correct, since the optimal chemotaxis phenotype is different in different environments[4], then we would expect that the shifts in the TB distribution during migration would depend on the environment that the population traverses. Past work has shown that, in liquid, cells with low TB climb chemical gradients faster[3], as long as their run durations are not longer than the time scale of rotational diffusion[24]. On the other hand, cells need to tumble more frequently to escape traps in porous media[4,22,25], thus we expect that higher TBs perform best in semisolid agarose.

To test this, we determined how the TB distributions of migrating populations shift after traveling through a liquid environment, without agarose (**Fig. 4a**). We again generated populations of *E. coli* with low and high average TB and propagated migrating waves with these populations, as well as the wild type, in capillary tubes filled with liquid media for 9 hours. aTc was pre-aged such that the media was 15 hours old at the end of the experiment, as above. We then isolated cells from the migrating populations and measured their TB distributions during migration.

When the population with high TB (initial mean TB = 0.32 ± 0.012) traveled through capillary tubes, its TB distribution shifted even lower (final mean TB = 0.16 ± 0.0062) compared to when it traveled through agarose swim plates (**Fig. 4e**). The enrichment of low-TB cells and filtering out of high-TB cells were much stronger in the capillary tubes (**Fig. 4h**) compared to the agarose swim plates (**Fig. 2h**). Transient degradation of aTc, alone, could not explain this shift to lower tumble biases, since the average TB among cells traveling in the wave was even lower than when cells were grown with the same concentration of fresh aTc in batch culture (**Fig. S2**). On the other hand, the TB distributions of the low-TB population (initial mean TB = 0.11 ± 0.011) shifted to slightly higher TBs when traveling through capillary tubes (final mean TB = 0.15 ± 0.029), but the shift in mean TB was not statistically significant (**Fig. 4c**). In this case, the enrichment of high-TB cells and filtering out of low-TB cells was weaker in the capillary tubes (**Fig. 4f**) compared to agarose swim plates (**Fig. 2f**). Even the WT population's TB distribution (initial mean TB = 0.22 ± 0.029) shifted to lower TB (final mean TB = 0.18 ± 0.01) during collective migration in liquid (**Fig. 4d,g**).

The low-TB population had the fastest expansion speed (mean expansion speed 3.96 ± 0.008 mm/min). Its TB distribution shifted the least during migration in capillary tubes, suggesting that its initial TB distribution was closest to the optimal tumbling phenotype for migration in liquid (**Methods; Fig. 4b**). The expansion speed of the WT population was statistically indistinguishable from this (3.86 ± 0.2 mm/min), and its initial TB distribution was also close to its traveling TB distribution. Finally, the high-TB population expanded slower than the other two populations (3.53 ± 0.004 mm/min).

Together, these results show that the shifts in TB distribution during collective migration of *E. coli* enrich for phenotypes with high chemotaxis performance, thus adapting the population to migrate through the current environment.

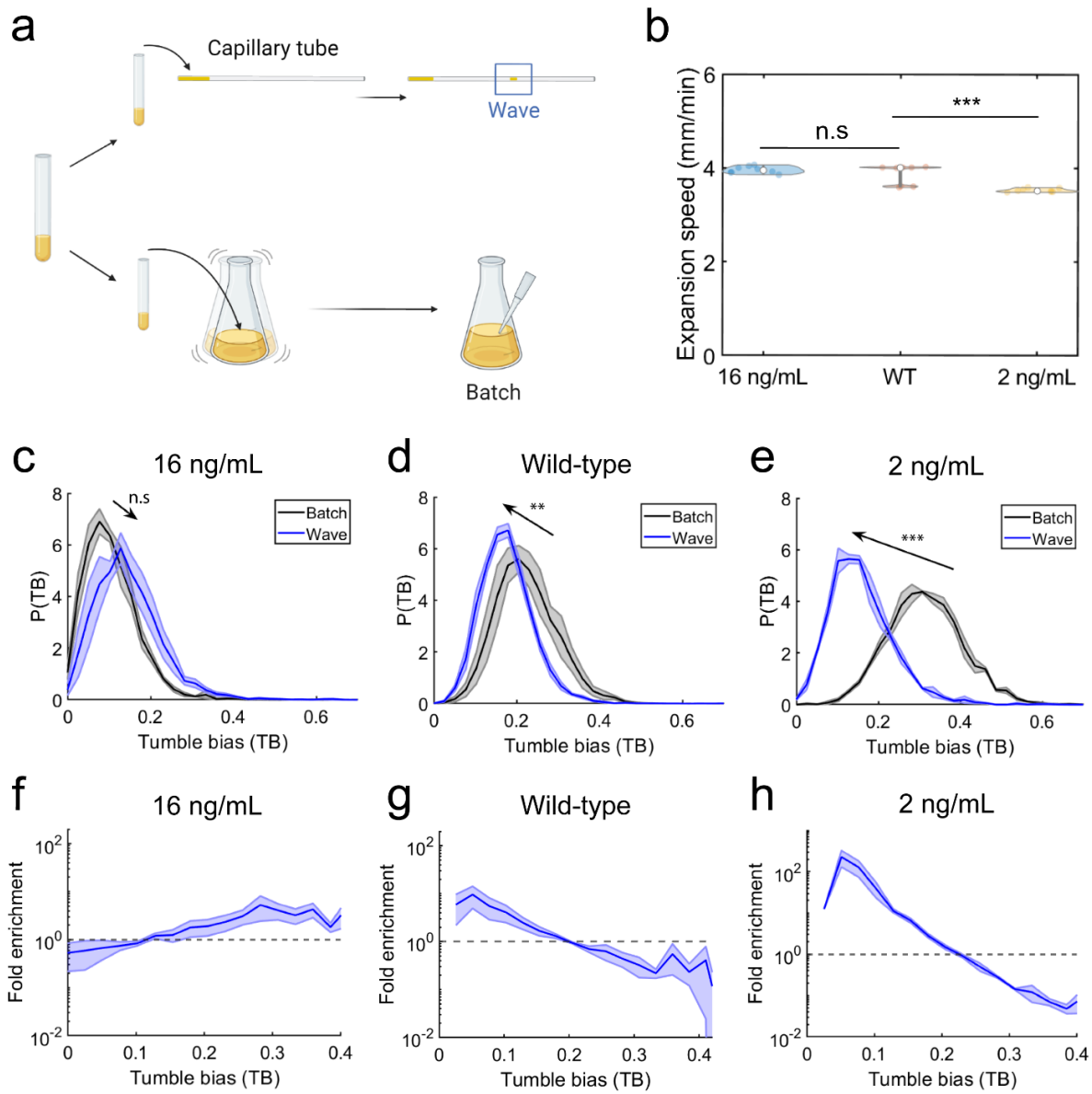

Figure 4. Tuning of TB distribution is different in liquid environment: (a) *Experimental design: a capillary tube and shaking flask containing the same amount of inducer are inoculated with the same initial population. TB distributions are measured and compared between batch and the migrating cells ("wave").* ***(b)*** *Expansion speeds of RP437 wild-type (mean 3.860 ± 0.02 mm/min; $N_{rep} = 5$), ΔcheZ (pTet-CheZ) induced with 2 ng/mL aTc (mean 3.530 ± 0.041 mm/min; $N_{rep} = 5$), and 16 ng/mL aTc (3.957 ± 0.007 mm/min; $N_{rep} = 5$) populations in capillary tubes.* ***(c)*** *In liquid, populations with low initial mean TB (mean TB = 0.10 ± 0.01; $N_{rep} = 3$, $N_{cells} = 21{,}891$) shift toward a higher mean TB (0.15 ± 0.03; $N_{rep} = 4$, $N_{cells} = 20{,}403$), but which is slightly lower than the mean TB in agarose swim plates (0.18 ± 0.004, as in Fig. 2c).* ***(d)*** *Unlike in agarose swim plates, wild-type population's TB distribution (0.22 ± 0.03; $N_{rep} = 3$, $N_{cells} = 9{,}417$) shifted toward a lower mean TB during collective migration in capillary tubes (0.18 ± 0.01; $N_{rep} = 5$, $N_{cells} = 16{,}768$) .* ***(e)*** *Populations with high initial mean TB (0.31 ± 0.01; $N_{rep} = 3$, $N_{cells} = 26{,}254$) shifted toward a lower mean TB (0.16 ± 0.01; $N_{rep} = 5$, $N_{cells} = 13{,}434$). The mean TB value is lower than what was observed during migration on agarose swim plates (0.23 ± 0.03, as in Fig. 2d).* ***(f)***

*For the migration of low TB populations, the fold enrichment is smaller than in agarose swim plates. ($N_{rep} = 3$) **(g).** Wild-type populations migrating in capillary tubes were enriched for low-TB cells ($N_{rep} = 3$), unlike what we observed when they migrated on agarose (Fig. 2g). **(f)** For high-TB populations, fold enrichment was stronger in capillary tubes compared to migration in agarose swim plates ($N_{rep} = 3$). More low-TB cells are enriched during migration in capillary tubes than on agarose plates (Fig. 2h).*

Collective migration tunes the population's distribution of sensing phenotypes to adapt to the chemical environment

Numerous phenotypic traits, in addition to tumble bias, affect a bacterium's chemotactic performance. If the tuning of TB distributions above were due to the enrichment of high-performing chemotaxis phenotypes, then we would expect enrichment to occur with *any* phenotype that impacts chemotactic performance. One such phenotype is the cell's sensing capability, which correlates with the abundances of its chemoreceptors[26,27]. *E. coli* express five chemoreceptor species, of which ~90% are either Tar, which binds with highest affinity to the amino acid L-aspartate, or Tsr, which binds with highest affinity to the amino acid L-serine[28-30]. Tsr is expressed separately from the chemotaxis operon[31], and thus its abundance can vary independently of other chemotaxis genes affecting chemotaxis performance. Therefore, we expect that Tsr would be enriched in a migrating wave that chases L-serine.

We measured the Tsr protein expression levels in populations of *E. coli* migrating on agarose swim plates with 100 μM L-aspartate or 100 μM L-serine as attractants, and no other amino acids (**Fig. 5a**). As a carbon source, we used glycerol because it is not an attractant[32]. To measure single-cell Tsr levels, we fused *tsr* on its native locus with mYFP, respectively (**Methods**). We used MG1655 as the parent strain here because, unlike RP437[31,33], it is not restricted by auxotrophic limitation and can grow in the presence of a single amino acid. Using fluorescent microscopy, we measured the average mYFP fluorescence in single cells picked from the edge of the migrating colonies and compared them to those grown in batch cultures supplemented with the same concentration of L-aspartate or L-serine (**Methods**).

The distributions of Tsr levels within the migrating populations on aspartate swim plates were similar to those grown in batch cultures, with the mean Tsr level statistically indistinguishable from batch culture (**Fig. 5b**; mean intensities $\langle \mathrm{Tsr} \rangle_{\mathrm{wave}} = 23.7 \pm 0.6\ \mu\mathrm{m}^{-2}$ and $\langle \mathrm{Tsr} \rangle_{\mathrm{batch}} = 27.2 \pm 3.84\ \mu\mathrm{m}^{-2}$). There was slight enrichment of intermediate Tsr levels (**Fig. 5c**), possibly because of the assistance Tsr provides to the adaptation of Tar (CheR and CheB can methylate and demethylate neighboring Tar receptors when bound to the pentapeptide of Tsr)[34,35]. In contrast, collective migration led to strong enrichment for cells with high levels of Tsr when the population chased serine (**Fig. 5d, e**; $\langle \mathrm{Tsr} \rangle_{\mathrm{wave}} = 53.6 \pm 6.6\ \mu\mathrm{m}^{-2}$ and $\langle \mathrm{Tsr} \rangle_{\mathrm{batch}} = 29.6 \pm 3.0\ \mu\mathrm{m}^{-2}$).

To confirm that the shift in the distribution of Tsr levels was not due to gene regulation, we employed an analogous strategy as the one described above for CheY and CheZ (**Fig. S5a**), but this time using a non-motile strain expressing fluorescently-labelled Tsr from its native locus (**Fig. S6a**). There were no differences in the Tsr levels among the non-motile cells, suggesting that there are negligible changes in *tsr* gene expression during collective migration (**Fig. S6b, c**). In addition, we found that Tsr levels are not regulated by serine or aspartate consumption when the amino acids are present in batch cultures at the same concentrations as in the swim plates (**Fig. S7**). This further indicates that the receptor enrichment that we measured after migration on swim plates is not a result of altered gene expression due to the presence of amino acids.

Taken together, these observations demonstrate that the tuning effect generalizes to sensory phenotypes: migrating populations can non-genetically adapt their distributions of receptor abundances, depending on the attractants they are chasing. Thus, collective migration when combined with growth enriches for multiple, continuous phenotypic traits and non-genetically adapts migrating populations to diverse environmental conditions.

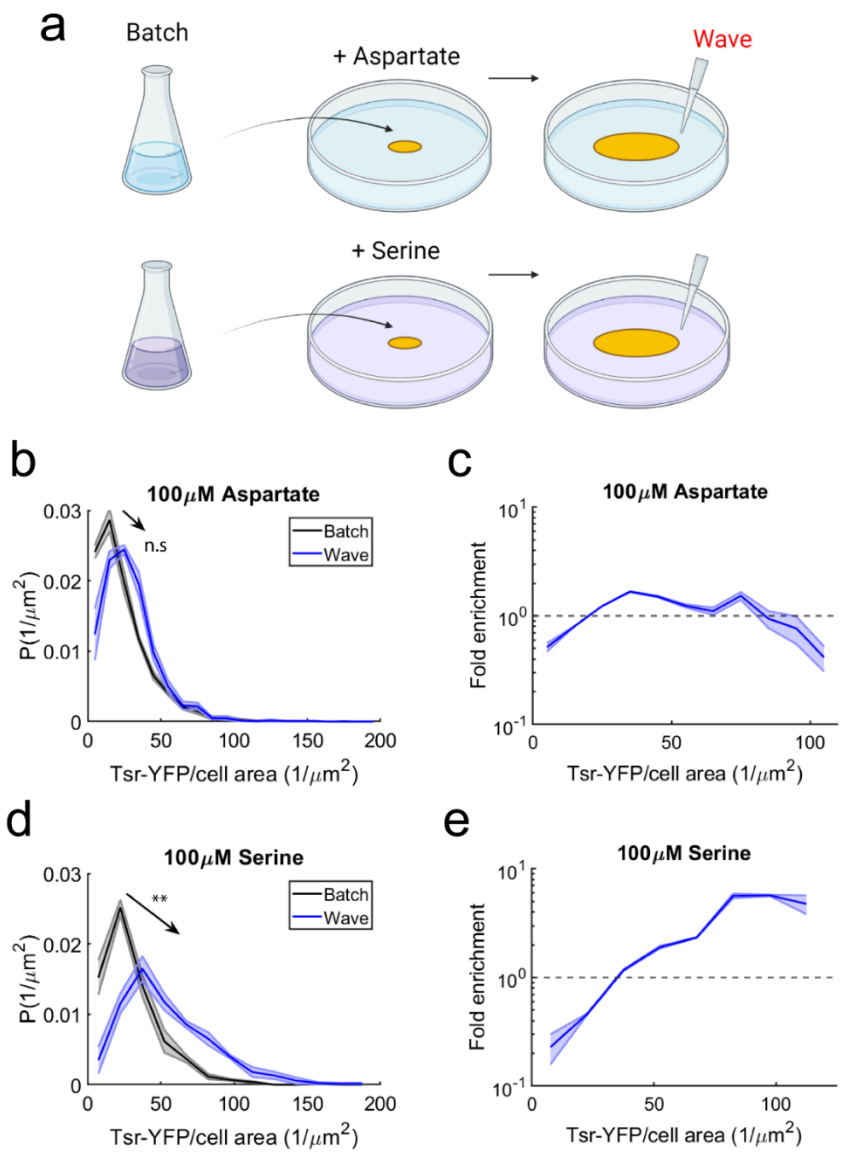

***Figure 5: Collective migration tunes the chemoreceptor levels depending on the attractants**. **(a)** Experimental design: E. coli MG1655 wild-type with YFP-labelled Tsr was inoculated on swim plates supplemented with 100 μM aspartate or 100 μM serine. The fluorescence of single cells was measured in populations at the edge of the migrating colonies ("wave") and in populations growing in batch culture. The single-cell fluorescence divided by the cell area is used as a proxy for receptor concentration. **(b)** Black is the distribution of Tsr levels of populations grown in batch culture with added aspartate (mean Tsr intensity = 23.7 ± 0.4 μm^{-2}; $N_{rep} = 3$, $N_{cells} = 2{,}076$), and blue is the distribution of Tsr levels of the migrating populations that chased aspartate (27.2 ± 3.8 μm^{-2}; $N_{rep} = 3$, $N_{cells} = 1{,}617$) . Shaded areas on*

the Tsr intensity distributions are the standard errors of the mean probabilities in each bin of intensity value. ***(c)*** *When chasing aspartate, the distributions of Tsr levels in migrating populations remained close to that in batch cultures, with only a weak fold increase in cells with intermediate Tsr levels and a weak fold decrease in cells with high Tsr levels. Shaded area on the fold-enrichment throughout is the standard errors of the mean enrichment values within each bin of Tsr intensity value.* ***(d)*** *Black is the distribution of Tsr levels of populations grown in batch culture with added serine (29.6 ± 2.9* μm^{-2}*;* $N_{rep} = 3$*,* $N_{cells} = 1{,}695$*), and blue is the distribution of Tsr levels of the migrating populations that chased serine (53.6 ± 6.5* μm^{-2}*;* $N_{rep} = 3$*,* $N_{cells} = 675$*).* ***e)*** *During collective migration on swim plates supplemented with serine, cells with higher Tsr levels are enriched for, and cells with lower Tsr levels are filtered out.*

Discussion

Here, we investigated how a population of cells regulates its distribution of phenotypes to migrate effectively in multiple environments. Using *E. coli* as a model system, we discovered that a migrating population can tune its distributions of swimming behaviors and sensing capabilities based on the physical and chemical properties of the environment. This tuning occurs dynamically and is explained by a theoretical model in which loss of low-performing chemotaxis phenotypes from the migrating front[1] balances the production of new phenotypes by growth[4,19]. This mechanism can act on top of the pre-existing variations of gene expression, but does not require *de novo* changes in gene expression or mutations. Adapting a continuous, multi-dimensional distribution of phenotypes enables the migrating population to enrich for fitter individuals based on the demands of the current environment. This allows it to maximize its expansion speed across a wide variety of potential environments.

We considered two phenotypes that impact chemotaxis performance: tumble bias and receptor abundance. However, we expect any phenotypic trait that contributes to chemotaxis performance will be enriched during collective migration. Surprisingly, there was no filtering of TB in wild-type RP437 populations during collective migration on agarose swim plates. Furthermore, both of the CheZ-inducible populations, with high or low initial mean TB, shifted toward the mean TB of the wild-type RP437 population (**Fig. S2).** Since collective migration enriches for high-performing phenotypes, this observation suggests that the TB distribution of wild-type RP437 populations is centered on optimal phenotypes for navigation in agar/agarose. Consistent with this, RP437 was originally selected for motility on agar swim plates and is a standard laboratory strain that has been used to study motility for decades[33,36]. However, RP437 is only one example of the diversity of *E. coli* swimming behavior. For example, the parent of RP437 uses a run-reverse mode and cannot expand in agarose swim plates[37]. To better understand the diverse colonization strategies employed by *E. coli* populations in the wild, it will be interesting to compare chemotaxis and motility across strains that inhabit different environments, such as ponds, soils, digestive tracts, or wounds.

Recent research emphasized the crucial role of emergent spatial structures during collective migration in enhancing genetic diversity within bacterial communities[38]. In traditional well-mixed environments, resource competition leads to the extinction of species with lower relative growth fitness[39]. However, during collective migration, species with lower relative growth fitness can coexist by competing for spatial territories rather than resources[16,38], enabling them to avoid extinction by colonizing specific habitats within the migrating colony. Furthermore, recent experiments demonstrated the evolution of mutants with different navigation capabilities from isogenic migrating populations[16], which implies that the emergent spatial organization of phenotypes can contribute to genetic diversity[1,20,40,41]. Together with our observation that the

environment determines the distribution of phenotypes that is enriched for, these results suggest that relative spatial arrangement of phenotypes within migrating groups may play an important role in eco-evolutionary dynamics.

Collective migration is not limited to bacteria: collective migration in which cells consume or degrade attractants to create and chase self-generated gradients is common in eukaryotic systems, including cancer and development[42,43]. Some examples are the migration of lateral line of zebrafish embryos[44], neural crest cells in *Xenopus laevis*[45], and melanoma cells[46]. The tuning of phenotypic distributions during collective migration only requires that some cells, due to having specific traits, to be better at navigating than others, therefore creating a "leader-follower" structure. Thus, diversity adaptation by collective migration may be a general strategy for cell populations to colonize diverse environments effectively.

Our results suggest that adaptation by collective behaviors can act on multiple continuous traits. By contrast, stochastic phenotype switching only acts on finite number of phenotypes, which limits the number of environmental properties that the population can respond to[5,7,47]. Altering gene expression consumes a significant percentage of the total proteome and energy budget, which can diminish overall growth temporarily due to proteome remodeling[18,48,49]. Moreover, evolution-driven adaptation to new environments can be slow and have trade-offs[50,51]. For example, under selection for fast expansion on swim plates, cells in recent experiments acquired mutations that enhanced their flagellar expression but exhibited slower growth[16,18]. Given the ubiquity of non-genetic diversity, we expect environment-dependent diversity adaptation by collective migration to be widespread in biology.

Methods

Strains, media, and growth conditions

All experiments were performed with *E. coli* K12 RP437 and MG1655 derivatives. To tune tumble bias distributions, we utilized an *E. coli* RP437 Δ*cheZ* strain that carries an aTc-inducible cassette of *cheZ* that is integrated in the chromosome at the *attB* site (RP437 Δ*cheZ pTet-cheZ*). To measure single cell Tsr receptor abundances, we utilized an *E. coli* MG1655 *ΔfliC:FLP* mutant (gift from Victor Sourjik) that has *tsr* translationally fused with monomeric YFP (A206K), on its native chromosomal locus (MG1655 Δ*fliC:FLP, tsr-mYFP*). To modulate motility in the previous strain, we transformed an arabinose-inducible plasmid expressing WT FliC (*pBad-fliC*, gift from Howard Berg) into MG1655 Δ*fliC:FLP, tsr-mYFP*. RP437 Δ*fliC* with CheY and CheZ translationally fused with mRFP and mYFP, respectively on their native chromosomal loci (RP437 Δ*fliC cheY-mRFP and cheZ-mYFP*) was used as a biosensor to measure expression of the *cheY* and *cheZ* genes in the swim plate assays. MG1655 Δ*fliC:FLP*, *tar-mCherry, tsr-mYFP*, was used as a biosensor to measure expression of the *tsr* gene. To insert genes on the native loci of the *E. Coli* chromosome, we employed the phage λ Red recombination system.

RP437-derived strains were stored as -80°C freezer DMSO-based stocks, and MG1655-derived strains were stored as glycerol-based stocks at the same temperature. M9 buffer supplemented with casamino acids, glycerol, and $MgSO_4$ (1x M9 salts, 0.4% v/v glycerol, 0.1% v/v casamino acids, 1mM $MgSO_4$) were used to grow RP437-derived strains. H1 minimal salts medium (MMH1: 50 mM KPO_4, 0.5 mM $MgSO_4$, 7.6 mM $(NH_4)_2SO_4$, 1.25 μM $Fe_2(SO_4)_3$) supplemented with 0.5% v/v glycerol and 0.01% w/v thiamine hydrochloride was used to grow MG1655-derived strains. To

436 grow overnight cultures, small inoculants from the freezer stocks were added into test tubes
437 containing 2 mL of media (with appropriate concentrations of inducers and antibiotics) in a shaking
438 incubator at 30°C rotating at 250 RPM. To grow day cultures for cell tracking experiments, RP437-
439 derived strain overnight cultures were diluted by 100-fold and re-grown in 5 mL of the appropriate
440 media until exponential phase (OD_{600} = 0.20). For receptor quantification experiments, MG1655-
441 derived strains were diluted 200-fold and re-grown in 10 mL of the appropriate media until
442 exponential phase (OD_{600} = 0.30). For cell tracking experiments, chemotaxis buffer (1x M9 buffer,
443 0.4% v/v glycerol, 0.010 mM methionine, 0.1 mM EDTA, and 0.1% v/v PVP-40) was used to wash
444 and dilute cells. For receptor quantification experiments, minimal chemotaxis buffer (10 mM KPO_4
445 and 0.1mM EDTA) was used to wash and dilute cells. For the TB measurements in batch cultures,
446 RP437 Δ*cheZ pTet-cheZ* were grown in media supplemented with aTc that was aged for 15 hours.

447

448 **Growth rates measurements**

449 Growth measurements were done using a microplate reader (BioTek Epoch 2 microplate
450 spectrophotometer). Overnight cultures were diluted by 100-fold into fresh media supplemented
451 with appropriate inducer concentrations. 200 µL of diluted cells were aliquoted into each well of
452 polystyrene 96-well plates (Falcon 96-wells REF 353072), and the plates were loaded into the
453 plate reader. The plates were incubated at 30°C while continuously shaking linearly at 567 cpm.
454 The OD_{600} of each well was measured every 7 minutes for 36 hours. To extract the growth rates
455 of each sample, the slopes of the linear region (at the mid-exponential growth phases) of the
456 natural log of OD_{600} versus time (hours) curves were calculated.

457

458 **Formation of propagating waves and expansion speed measurements using swim plate**
459 **and capillary tube assays**

460 For the swim plate assay, 3 µL of cells in exponential phase were inoculated at the center of semi-
461 solid agarose plates for RP437-derived strains or 10 μL of cells in exponential phase for MG1655-
462 derived strains. For RP437-derived strains, the semi-solid agarose plates were made using M9-
463 based media, as described above, supplemented with 0.14% agarose (American Bioanalytical
464 Agarose GPG/LE) and appropriate concentrations of aTc. Similarly, for MG1655-derived strains,
465 the semi-solid agarose plates were made using H1 minimal media, as described above,
466 supplemented with 0.14% agarose. The plates were incubated at 30°C for 15 hours (RP437-
467 derived strains) or at 33.5°C for 48 hours (MG1655-derived strains). The edges of the migrating
468 colonies were picked using pipette tips and diluted into chemotaxis buffer (for RP437-derived
469 strains) or minimal chemotaxis buffer (for MG1655-derived strains) for subsequent tracking and
470 imaging analyses. To measure the expansion speeds of bacterial populations in swim plates,
471 images were taken with a Canon DS126291 camera every 30 minutes. The diameters of the
472 expansion rings as a function of time and expansion speeds were extracted from the images using
473 a customized MATLAB code.

474 For the capillary tube assay, the protocol was adapted from previous work [14]. Overnight cultures
475 were inoculated 100-fold into 5 mL of media with appropriate inducers and grown at 30°C until
476 OD_{600} = 0.2. Cells were concentrated to an OD_{600} = 6. A 12-inch capillary tube was filled with
477 growth media (M9 glycerol with casamino acids, $MgSO_4$, and PVP-40) and 6-hours aged aTc,
478 and one side of the tube was plugged by stabbing the tube into a plate filled with solidified agar

479 (1.5% agar in distilled water). The concentrated cell mixture was filled on the other side of the
480 tube using a 1 mL syringe, and another agar plug was added into that side. Both sides of the tube
481 were then plugged with clay. The tubes are incubated horizontally at 30°C for 9 hours. To isolate
482 the wave, a 3-cm section of the tube that contained the wave was fractionated, and the mixture
483 inside the 3-cm section was diluted into chemotaxis buffer for subsequent tracking analysis. To
484 measure the expansion speeds of bacterial populations in capillary tubes, images were taken with
485 a Canon DS126291 camera every 10 minutes. Positions of the populations as a function of time
486 and expansion speeds were extracted from images using ImageJ.

487

488 **Microfluidic device preparation**

489 To track single cell swimming behavior, we utilized a rectangular channel microfluidic device (0.5
490 mm wide, 30 mm long, and 60 μm deep). The device was constructed from PDMS with standard
491 lithography methods. To cast the device, a pre-prepared mold was coated with a 5-mm thick layer
492 of degassed 10:1 PDMS-to-curing agent mixture (Sylgard 184, Dow Chemical). The mold was
493 then baked at 70°C for 12 hours. Devices were cut out of the mold, and a hole was punched using
494 a 20-gauge blunt-tip needle on each side of the channel. The device was rinsed with isopropanol,
495 methanol, and water. A 22 mm x 50 mm glass coverslip was rinsed with acetone, isopropanol,
496 methanol, and water. The coverslip and device were then treated inside a plasma cleaner for 1
497 minute and bonded together. The bonded device was heated at 80°C for 15 minutes and cooled
498 to room temperature before cells were injected inside.

499

500 **Tracking single cells and tumble detection**

501 Washed cells were diluted with chemotaxis buffer to an OD_{600} = 0.0005. The diluted mixture was
502 injected inside the microfluidic device using a 1 mL syringe. To prevent evaporation, holes on
503 both sides of the microfluidic device were taped. The device was placed on an inverted
504 microscope (Nikon Eclipse Ti-U) equipped with a custom environmental chamber (50% humidity
505 and 30°C). A custom MATLAB script was used to record 3-minute phase contrast videos at 4X
506 magnification and 20 frames-per-second. Data from video recordings were stored as .bin files.

507 A customized MATLAB code was used to detect tumble and extract tumble bias of single cells,
508 as previously described[52]. Only trajectories longer than 10 seconds were considered for analysis.
509 Each tumble bias distribution was generated using 4 3-minute videos that contained ~1000 total
510 trajectories.

511

512 **Protein expression measurements in swim plates**

513 Non-motile MG1655-derived cells expressing labeled Tsr or non-motile RP437-derived cells
514 expressing labeled CheY and CheZ used as biosensors for gene expression were grown as
515 described above. Subsequently, cells were mixed with the appropriate media and 0.14% liquified
516 agarose to a final OD_{600} = 0.01. Swim plates were left to solidify at room temperature for 2-3
517 hours, and afterward, 10 µL of OD_{600} = 0.01 motile WT MG1655 or motile WT RP437 cells were
518 inoculated in the center of the plate. The motile population of cells shapes the gradient of the plate
519 and ensures that the non-motile biosensor strain experiences the same local environment as

motile cells. After a colony of migrating cells has formed, cells from the center and the edge of the colony are picked and diluted into minimal chemotaxis buffer for subsequent imaging.

Single-cell protein copy number quantification using fluorescent microscopy

Washed cells were diluted 10-fold and plated on agarose pads (3% agarose in minimal chemotaxis buffer). The cell suspension was left to dry for 10 minutes, and cells were immediately imaged afterward. Imaging was performed using an inverted microscope (Nikon Eclipse Ti-E) equipped with an oil immersion 100x phase-contrast objective lens. To measure the fluorescence intensity of the strain expressing cheY-mRFP and cheZ-mYFP, fluorescent proteins were excited using a light-emitting diode illumination system (pE-4000, CoolLED). The RFP and YFP channels were imaged consecutively using a multi-band filter (Semrock), and the fluorescence emissions were led into a 2-camera image splitter (TwinCam, Cairn), leading to two identical sCMOS cameras (ORCA-Flash4.0 V2, Hamamatsu). The same setup was used to measure the fluorescence intensity of the strain expressing Tsr-mYFP. In a typical experiment, 20 fields of view, containing approximately 1000 cells in total, are imaged.

Fluorescent image analysis for protein copy number quantification

For each field of view, one phase contrast, one YFP, and one RFP channel images were acquired. Using a custom MATLAB script, images from the two cameras were aligned using an affine transformation, and cells were segmented on the phase-contrast channel using a modified Otsu algorithm. Then, the image background was subtracted from each image, and the fluorescent intensity of every cell was extracted. Finally, the area of each cell was calculated by fitting an ellipsoid. The fluorescent intensity of each cell was divided by the cell area as a measure of protein concentration.

Reproducibility and statistical analysis

All experiments reported in this work were repeated at least 3 times. All measurement values of TB, expansion speeds, growth rates, protein levels were reported as the average of the means of the distributions across biological replicates. Uncertainties in these average values were reported as the standard deviation of the means of the distributions.

To construct the TB distributions, TB values were sorted into bins, and the probability density were normalized by dividing the trajectory time within each bin by the total trajectory time. To represent the variations in TB distributions, the standard error of the mean TBs within each bin was calculated. Similarly, with the Tsr intensity distribution, single-cell Tsr intensities were sorted into bins, and the probability density in each bin was calculated. The variations in Tsr intensity distributions are represented as the standard error of the mean intensities within each bin.

To construct the fold-enrichment curve, the probability density values of each TB or Tsr intensity bins observed in the distributions during collective migration were divided by the values observed in batch cultures. Variations in fold-enrichments are represented as the standard error of the mean fold-enrichment values within each bin.

To determine statistical significance between TB and protein level distributions, two-sided T-test was performed on the mean values. Similarly, two-sided T-test was performed to determine significance of growth rates and expansion speeds between experiments.

Analysis code and data availability

Analysis code will be uploaded to the Emonet lab GitHub (github.com/emonetlab) upon publication. Data will be made available on datadryad.org upon publication.

Acknowledgments: We thank Jing Yan, Amir Pahlavan, and Jeremy Moore for useful discussions. We thank Simone Boskamp for assistance with cloning and Cherin Mohamed for assistance with experiments. We thank Victor Sourjik and Howard Berg for providing plasmids and strains that were important for this work.

Funding: This work was supported by NIH awards R01GM138533 and R01GM106189. Lam Vo is supported by NIH F31GM149174-01.

References

1 Fu, X. *et al.* Spatial self-organization resolves conflicts between individuality and collective migration. *Nat Commun* **9**, 2177 (2018). https://doi.org:10.1038/s41467-018-04539-4

2 Huh, D. & Paulsson, J. Non-genetic heterogeneity from stochastic partitioning at cell division. *Nat Genet* **43**, 95-100 (2011). https://doi.org:10.1038/ng.729

3 Waite, A. J. *et al.* Non-genetic diversity modulates population performance. *Mol Syst Biol* **12**, 895 (2016). https://doi.org:10.15252/msb.20167044

4 Mattingly, H. H. & Emonet, T. Collective behavior and nongenetic inheritance allow bacterial populations to adapt to changing environments. *Proc Natl Acad Sci U S A* **119**, e2117377119 (2022). https://doi.org:10.1073/pnas.2117377119

5 Norman, T. M., Lord, N. D., Paulsson, J. & Losick, R. Stochastic Switching of Cell Fate in Microbes. *Annu Rev Microbiol* **69**, 381-403 (2015). https://doi.org:10.1146/annurev-micro-091213-112852

6 Kussell, E. & Leibler, S. Phenotypic diversity, population growth, and information in fluctuating environments. *Science* **309**, 2075-2078 (2005). https://doi.org:10.1126/science.1114383

7 Balaban, N. Q., Merrin, J., Chait, R., Kowalik, L. & Leibler, S. Bacterial persistence as a phenotypic switch. *Science* **305**, 1622-1625 (2004). https://doi.org:10.1126/science.1099390

8 Kussell, E., Kishony, R., Balaban, N. Q. & Leibler, S. Bacterial persistence: a model of survival in changing environments. *Genetics* **169**, 1807-1814 (2005). https://doi.org:10.1534/genetics.104.035352

9 Wood, T. K., Knabel, S. J. & Kwan, B. W. Bacterial persister cell formation and dormancy. *Appl Environ Microbiol* **79**, 7116-7121 (2013). https://doi.org:10.1128/AEM.02636-13

10 Oren, Y. *et al.* Cycling cancer persister cells arise from lineages with distinct programs. *Nature* **596**, 576-582 (2021). https://doi.org:10.1038/s41586-021-03796-6

11 Bressloff, P. C. Stochastic switching in biology: from genotype to phenotype. *J. Phys. A: Math. Theor.* **50** (2017).

12 Tian, T. & Burrage, K. Stochastic models for regulatory networks of the genetic toggle switch. *Proc Natl Acad Sci U S A* **103**, 8372-8377 (2006). https://doi.org:10.1073/pnas.0507818103

13 Chan, B. K. *et al.* Phage selection restores antibiotic sensitivity in MDR Pseudomonas aeruginosa. *Sci Rep* **6**, 26717 (2016). https://doi.org:10.1038/srep26717

14 Poole, K. Outer membranes and efflux: the path to multidrug resistance in Gram-negative bacteria. *Curr Pharm Biotechnol* **3**, 77-98 (2002). https://doi.org:10.2174/1389201023378454

15 Schmitt, M. W., Loeb, L. A. & Salk, J. J. The influence of subclonal resistance mutations on targeted cancer therapy. *Nat Rev Clin Oncol* **13**, 335-347 (2016). https://doi.org:10.1038/nrclinonc.2015.175

16 Liu, W., Cremer, J., Li, D., Hwa, T. & Liu, C. An evolutionarily stable strategy to colonize spatially extended habitats. *Nature* **575**, 664-668 (2019). https://doi.org:10.1038/s41586-019-1734-x

17 Fraebel, D. T. *et al.* Environment determines evolutionary trajectory in a constrained phenotypic space. *Elife* **6** (2017). https://doi.org:10.7554/eLife.24669

18 Ni, B. *et al.* Evolutionary Remodeling of Bacterial Motility Checkpoint Control. *Cell Rep* **18**, 866-877 (2017). https://doi.org:10.1016/j.celrep.2016.12.088

19 Pleska, M., Jordan, D., Frentz, Z., Xue, B. & Leibler, S. Nongenetic individuality, changeability, and inheritance in bacterial behavior. *Proc Natl Acad Sci U S A* **118** (2021). https://doi.org:10.1073/pnas.2023322118

20 Cremer, J. *et al.* Chemotaxis as a navigation strategy to boost range expansion. *Nature* **575**, 658-663 (2019). https://doi.org:10.1038/s41586-019-1733-y

21 Zheng, H. *et al.* Interrogating the Escherichia coli cell cycle by cell dimension perturbations. *Proc Natl Acad Sci U S A* **113**, 15000-15005 (2016). https://doi.org:10.1073/pnas.1617932114

22 Wolfe, A. J. & Berg, H. C. Migration of bacteria in semisolid agar. *Proc Natl Acad Sci U S A* **86**, 6973-6977 (1989). https://doi.org:10.1073/pnas.86.18.6973

23 Staropoli, J. F. & Alon, U. Computerized analysis of chemotaxis at different stages of bacterial growth. *Biophys J* **78**, 513-519 (2000). https://doi.org:10.1016/S0006-3495(00)76613-6

24 Dufour, Y. S., Fu, X., Hernandez-Nunez, L. & Emonet, T. Limits of feedback control in bacterial chemotaxis. *PLoS Comput Biol* **10**, e1003694 (2014). https://doi.org:10.1371/journal.pcbi.1003694

25 Licata, N. A., Mohari, B., Fuqua, C. & Setayeshgar, S. Diffusion of Bacterial Cells in Porous Media. *Biophys J* **110**, 247-257 (2016). https://doi.org:10.1016/j.bpj.2015.09.035

26 Tu, Y., Shimizu, T. S. & Berg, H. C. Modeling the chemotactic response of Escherichia coli to time-varying stimuli. *Proc Natl Acad Sci U S A* **105**, 14855-14860 (2008). https://doi.org:10.1073/pnas.0807569105

27 Keegstra, J. M. *et al.* Phenotypic diversity and temporal variability in a bacterial signaling network revealed by single-cell FRET. *Elife* **6** (2017). https://doi.org:10.7554/eLife.27455

28 Salman, H. & Libchaber, A. A concentration-dependent switch in the bacterial response to temperature. *Nat Cell Biol* **9**, 1098-1100 (2007). https://doi.org:10.1038/ncb1632

29 Yang, Y. *et al.* Relation between chemotaxis and consumption of amino acids in bacteria. *Mol Microbiol* **96**, 1272-1282 (2015). https://doi.org:10.1111/mmi.13006

30 Li, M. & Hazelbauer, G. L. Cellular stoichiometry of the components of the chemotaxis signaling complex. *J Bacteriol* **186**, 3687-3694 (2004). https://doi.org:10.1128/JB.186.12.3687-3694.2004

31 Blattner, F. R. *et al.* The complete genome sequence of Escherichia coli K-12. *Science* **277**, 1453-1462 (1997). https://doi.org:10.1126/science.277.5331.1453

32 Adler, J., Hazelbauer, G. L. & Dahl, M. M. Chemotaxis toward sugars in Escherichia coli. *J Bacteriol* **115**, 824-847 (1973). https://doi.org:10.1128/jb.115.3.824-847.1973

33 Parkinson, J. S. & Houts, S. E. Isolation and behavior of Escherichia coli deletion mutants lacking chemotaxis functions. *J Bacteriol* **151**, 106-113 (1982). https://doi.org:10.1128/jb.151.1.106-113.1982

34 Endres, R. G. & Wingreen, N. S. Precise adaptation in bacterial chemotaxis through "assistance neighborhoods". *Proc Natl Acad Sci U S A* **103**, 13040-13044 (2006). https://doi.org:10.1073/pnas.0603101103

35 Sourjik, V. Receptor clustering and signal processing in E. coli chemotaxis. *Trends Microbiol* **12**, 569-576 (2004). https://doi.org:10.1016/j.tim.2004.10.003

36 Parkinson, J. S. cheA, cheB, and cheC genes of Escherichia coli and their role in chemotaxis. *J Bacteriol* **126**, 758-770 (1976). https://doi.org:10.1128/jb.126.2.758-770.1976

37 Kinosita, Y. *et al.* Distinct chemotactic behavior in the original Escherichia coli K-12 depending on forward-and-backward swimming, not on run-tumble movements. *Sci Rep* **10**, 15887 (2020). https://doi.org:10.1038/s41598-020-72429-1

38 Gude, S. *et al.* Bacterial coexistence driven by motility and spatial competition. *Nature* **578**, 588-592 (2020). https://doi.org:10.1038/s41586-020-2033-2

39 Goldford, J. E. *et al.* Emergent simplicity in microbial community assembly. *Science* **361**, 469-474 (2018). https://doi.org:10.1126/science.aat1168

40 Bai, Y. *et al.* Spatial modulation of individual behaviors enables an ordered structure of diverse phenotypes during bacterial group migration. *Elife* **10** (2021). https://doi.org:10.7554/eLife.67316

41 Zuo, W. & Wu, Y. Dynamic motility selection drives population segregation in a bacterial swarm. *Proc Natl Acad Sci U S A* **117**, 4693-4700 (2020). https://doi.org:10.1073/pnas.1917789117

42 Venkiteswaran, G. *et al.* Generation and dynamics of an endogenous, self-generated signaling gradient across a migrating tissue. *Cell* **155**, 674-687 (2013). https://doi.org:10.1016/j.cell.2013.09.046

43 Scherber, C. *et al.* Epithelial cell guidance by self-generated EGF gradients. *Integr Biol (Camb)* **4**, 259-269 (2012). https://doi.org:10.1039/c2ib00106c

44 David, N. B. *et al.* Molecular basis of cell migration in the fish lateral line: role of the chemokine receptor CXCR4 and of its ligand, SDF1. *Proc Natl Acad Sci U S A* **99**, 16297-16302 (2002). https://doi.org:10.1073/pnas.252339399

45 Theveneau, E. & Mayor, R. Neural crest delamination and migration: from epithelium-to-mesenchyme transition to collective cell migration. *Dev Biol* **366**, 34-54 (2012). https://doi.org:10.1016/j.ydbio.2011.12.041

46 Muinonen-Martin, A. J. *et al.* Melanoma cells break down LPA to establish local gradients that drive chemotactic dispersal. *PLoS Biol* **12**, e1001966 (2014). https://doi.org:10.1371/journal.pbio.1001966

47 Acar, M., Mettetal, J. T. & van Oudenaarden, A. Stochastic switching as a survival strategy in fluctuating environments. *Nat Genet* **40**, 471-475 (2008). https://doi.org:10.1038/ng.110

48 Erickson, D. W. *et al.* A global resource allocation strategy governs growth transition kinetics of Escherichia coli. *Nature* **551**, 119-123 (2017). https://doi.org:10.1038/nature24299

49 Scott, M. & Hwa, T. Shaping bacterial gene expression by physiological and proteome allocation constraints. *Nat Rev Microbiol* **21**, 327-342 (2023). https://doi.org:10.1038/s41579-022-00818-6

50 Barbosa, C., Romhild, R., Rosenstiel, P. & Schulenburg, H. Evolutionary stability of collateral sensitivity to antibiotics in the model pathogen Pseudomonas aeruginosa. *Elife* **8** (2019). https://doi.org:10.7554/eLife.51481

51 Burmeister, A. R. *et al.* Pleiotropy complicates a trade-off between phage resistance and antibiotic resistance. *Proc Natl Acad Sci U S A* **117**, 11207-11216 (2020). https://doi.org:10.1073/pnas.1919888117

52 Mattingly, H. H., Kamino, K., Machta, B. B. & Emonet, T. Escherichia coli chemotaxis is information limited. *Nat Phys* **17**, 1426-1431 (2021). https://doi.org:10.1038/s41567-021-01380-3